Analysis of the ^{57}Fe Hyperfine Coupling Constants and Spin States in Nitrogenase P-Clusters

J.-M. Mouesca,*,† L. Noodleman,* and D. A. Case

Department of Molecular Biology, The Scripps Research Institute, La Jolla, California 92037

Received January 21, 1994[⊗]

We present a new analysis of the EPR data and Mössbauer parameters of the redox state P^{OX} of the P-cluster of nitrogenase. In our model, each half of the cluster is formally equivalent to a "classic" $[Fe_4S_4]^+$ unit containing one ferric and three ferrous ions. However, due to the presence of an additional serine ligand at one iron site, the spin properties of the two halves are distinct; one has a typical spin $S_1 = {}^1/_2$ and the other, close to the serine, a spin $S_2 = {}^7/_2$ (we considered also the case $S_2 = {}^5/_2$). A parallel coupling of these two subspins (resulting in the state $|S_1, S_2, S_t\rangle$ with S_t equal to 4) is found to be more likely than the antiparallel $|{}^1/_2, {}^7/_2, 3\rangle$. This conclusion is based on two lines of evidence. First, the ferrous ions (identified from their large isomer shifts) present both positive and negative hyperfine parameters, which points to a ferromagnetic coupling of the two cubane subspins S_1 and S_2. Second, we propose the use of a simple empirical quantity $a_{test} \equiv \sum A_{iz}$, where A_{iz} are the measured hyperfine parameters for P^{OX}. Comparison of the values of a_{test} (which is markedly S_t-dependent) for P-clusters from *Clostridium pasteurianum* (Cp) and from *Azotobacter vinelandii* (Av) with theoretical estimates for the possible parallel-coupled states $|{}^1/_2, {}^5/_2, 3\rangle$ and $|{}^1/_2, {}^7/_2, 4\rangle$ clearly favors the latter. Our spin coupling model predicts a 5:3 (5 negative and 3 positive) pattern for the hyperfine parameters rather than 4:4 as originally measured in Av or 6:2 as in Cp (and also in Av after experimental reanalysis). This model for the P^{OX} state is combined with other information to provide a consistent picture of oxidation states and spin coupling patterns in all four observed P-cluster redox states.

I. Introduction

Nitrogenases catalyze one of the most important synthetic processes found in nature, the reduction of N_2 to NH_3. Much effort has been directed toward obtaining a better knowledge of the structure of the active sites involved. Recently, a crystallographic structure of the FeMo protein of the nitrogenase from *Azotobacter vinelandii* at 2.7 and 2.2 Å resolution has been reported.[1,2] The FeMo protein is composed of four subunits in an $\alpha_2\beta_2$ arrangement. The current active-site model contains two Mo centers (FeMo cofactors with one Mo, seven irons, and one homocitrate) and two P-clusters (each made of two 4Fe4S clusters bridged by two cysteines and also (probably) by a disulfide ligand). Starting from the resting native protein (with $S = {}^3/_2$),[3] an initial four-electron oxidation preserves the $S = {}^3/_2$ signal, but a further oxidation by two electrons results in the disappearance of this $S = {}^3/_2$ signal.[4] This whole process appears to correspond to an initial oxidation of the P-clusters (from P^N to P^{OX} with two electrons per (8Fe) cluster converting an EPR-silent ($S = 0$) state to a non-Kramers[5] species of spin $S_t = 3$ or 4) followed by second oxidation of the FeMo clusters (from M^N with spin ${}^3/_2$ to the EPR-silent M^{OX}) as depicted below[4,5] (here for one cluster of each type):

$$\begin{cases} P^N(S_t = 0) \\ M^N(S = {}^3/_2) \end{cases} \overset{2e^-}{\rightleftharpoons} \begin{cases} P^{OX}(S_t = 3 \text{ or } 4) \\ M^N(S = {}^3/_2) \end{cases} \overset{1e^-}{\rightleftharpoons} \begin{cases} P^{OX}(S_t = 3 \text{ or } 4) \\ M^{OX}(S = 0) \end{cases}$$

The P-cluster is composed of eight iron atoms (formally a mixture of high-spin ferrous and ferric ions) and is described therefore as a mixed-valence system. It will be shown in this paper that both localized $Fe^{2+}-Fe^{3+}$ and delocalized $Fe^{2.5+}-Fe^{2.5+}$ dimer configurations can be encountered as components of the larger cluster. As with other biological iron-sulfur clusters, the P-cluster is a spin-coupled system in which relatively strong antiferromagnetic interactions occur between the metal sites, mediated by bridging (sulfur) ligands. In the general case of dimers (or polynuclear iron−sulfur systems), the observed hyperfine parameters $A(Fe_i)$ are a measure of the strength of the interaction between the nuclear spin of the iron ions and the *total* electron spin S_t of the system. In the case of a monomeric system (as in rubredoxins) the electronic spin is ${}^5/_2$ for Fe^{3+} and 2 for Fe^{2+} and the hyperfine parameter is denoted as $a(Fe_i)$. Since in a polynuclear iron−sulfur system the iron sites are high-spin, the cluster can be considered as made of monomer spins S_i strongly coupled to the total spin S_t. Hyperfine measurements thus yield $A(Fe_i)$ (referred to S_t) rather than $a(Fe_i)$ (referred to S_i). These quantities are related:

$$A(Fe_i) = K_i a(Fe_i) \tag{1}$$

The constant of proportionality K_i is a spin projection coefficient describing the projection of the local spin S_i onto the total spin S_t:

$$K_i = \langle S_{iz}\rangle / \langle S_{tz}\rangle \tag{2}$$

K_i can be determined by expanding the total spin wave function (coupled representation) in terms of product states of the individual irons (uncoupled representation) using the

† Present address: DRFMC/SESAM/SCPM, Centre d'Etudes Nucléaires de Grenoble, 85 X 38041 Grenoble, France.

⊗ Abstract published in *Advance ACS Abstracts,* September 15, 1994.

(1) Kim, J.; Rees, D. C. *Science* **1992**, *257*, 1677−1682.
(2) Chan, M. K.; Kim, J.; Rees, D. C. *Science* **1993**, *260*, 792−794.
(3) Munck, E.; Rhodes, H.; Orme-Johnson, W. H.; Davis, L. C.; Brill, W. J.; Shah, V. K. *Biochim. Biophys. Acta* **1975**, *400*, 32−53.
(4) Zimmermann, R.; Munck, E.; Brill, W. J.; Shah, V. K.; Henzl, M. T.; Rawlings, J.; Orme-Johnson, W. H. *Biochim. Biophys. Acta* **1978**, *537*, 185−207.
(5) Surerus, K. K.; Hendrich, M. P.; Christie, P. D.; Rottgardt, D.; Orme-Johnson, W. H.; Munck, E. *J. Am. Chem. Soc.* **1992**, *114*, 8579−8590.

0020-1669/94/1333-4819$04.50/0

Wigner–Eckart theorem.[6] This approach was originally applied to 2Fe reduced ferredoxins[7] and then extended to other systems like 2Fe and 3Fe systems in general,[8] 3Fe ferredoxins (both oxidized[9-11] and reduced[12]), and 4Fe ferredoxins (oxidized[13b,14] and reduced[13a,15]). It is also useful to consider the case for which a system of net total S_t can be decomposed into two or more subunits of spin S_q which couple to S_t ($\sum \vec{S}_q = \vec{S}_t$). A common example is the analysis of 4Fe iron-sulfur cubanes in terms of 2Fe dimers. Within each subunit q, one can define a spin projection coefficient K_i^q as the projection of the local site spin i onto the spin S_q of the subunit q:

$$K_i^q = \langle S_{iz}\rangle / \langle S_{qz}\rangle \tag{3}$$

Each subunit spin S_q can be then projected onto the total spin S_t of the cluster, resulting in another set of spin coefficients $\{K^q\}_{q=1,2}$:

$$K^q = \langle S_{qz}\rangle / \langle S_{tz}\rangle \tag{4}$$

Evidently we have the following relation between K_i, K_i^q, and K^q holding in general:

$$K_i = [\langle S_{iz}\rangle / \langle S_{qz}\rangle][\langle S_{qz}\rangle / \langle S_{tz}\rangle] = K_i^q K^q \tag{5}$$

Here we apply this sort of analysis to the MoFe protein of nitrogenase, confining our discussion to the P-cluster and in particular to its P^{OX} oxidation state for which Mössbauer measurements of the ^{57}Fe hyperfine coupling constants are available.[4,16] We use their signs and magnitudes to provide clues about the nature of the spin-coupling in that redox state. The experimental measurements have been analyzed on the basis of a magnetically uniaxial character of the electronic ground state of P^{OX}. The magnetic hyperfine tensors were assumed to have the same principal axis system as the zero-field splitting (ZFS) term. Consequently, the measured internal field H_{int}^i is related to the hyperfine tensor $A(Fe_i)$ (or more precisely the projection of that tensor onto the z-axis of the ZFS tensor, A_{iz}) through the relation: $H_{int}^i = -\langle S_{tz}\rangle A_{iz}/g_n\beta_n$. The magnetic hyperfine interaction is hence characterized by an internal magnetic field H_{int} aligned along that z-axis.[4,5] For sufficiently large applied magnetic fields (>20 kG) the system is essentially in the state for which $\langle S_{tz}\rangle = -S_t$, so that $H_{int}^i = +S_t A_{iz}/g_n\beta_n$ and the measured internal fields have the same signs as their corresponding hyperfine couplings.[4] From now on we will always refer to this last expression for the internal fields. Our theoretical calculations of hyperfine coupling constants will be based on the use of *isotropic* site values $a(Fe_i)$. For 4Fe systems the measured hyperfine tensors are nearly isotropic to a good approximation: the anisotropy represents about ±16% (at most) of the isotropic values for the $[Fe_4S_4]^+$ cluster in aconitase[17] and about ±10% (at most) for a $[Fe_4S_4]^{3+}$ synthetic cluster,[18] so that we can safely compare our theoretical predictions with the measured A_z for P^{OX}.

Table 1. Summary of Likely Oxidation and Spin States of P-Clusters

name of state[a]	formal iron oxidn states	2[Fe$_4$S$_4$] analogue[b] core oxidn states		tot. spin
P^N	$(4Fe^{2+})$, $(4Fe^{2+})$	$[Fe_4S_4]^0$	$[Fe_4S_4]^0$	
		$S_1 = 0$	$S_2 = 0$	$S_t = 0$
P^{pOX}	$(2Fe^{2+}, 2Fe^{2.5+})$, $(4Fe^{2+})$	$[Fe_4S_4]^+$	$[Fe_4S_4]^0$	
		$S_1 = 1/2$	$S_2 = 0$	$S_t = 1/2$
	$(4Fe^{2+})$, $(3Fe^{2+}, 1Fe^{3+})$	$[Fe_4S_4]^0$	$[Fe_4S_4]^+$	
		$S_1 = 0$	$S_2 = 5/2$	$S_t = 5/2$
P^{OX}	$(2Fe^{2+}, 2Fe^{2.5+})$, $(3Fe^{2+}, 1Fe^{3+})$	$[Fe_4S_4]^+$	$[Fe_4S_4]^+$	
		$S_1 = 1/2$	$S_2 = 7/2$	$S_t = 3$ or 4
		$S_1 = 1/2$	$S_2 = 5/2$	$S_t = 3$
P^{sOX}	$(4Fe^{2.5+})$, $(3Fe^{2+}, 1Fe^{3+})$	$[Fe_4S_4]^{2+}$	$[Fe_4S_4]^+$	
		$S_1 = 0$	$S_2 = 7/2$	$S_t = 7/2$
	$(2Fe^{2+}, 2Fe^{2.5+})$, $(4Fe^{2.5+})$	$[Fe_4S_4]^+$	$[Fe_4S_4]^{2+}$	
		$S_1 = 1/2$	$S_2 = 0$	$S_t = 1/2$

[a] An alternative notation has been proposed: P^0, P^{1+}, P^{2+}, and P^{3+}, respectively.[22] [b] "Analogue" oxidation states are derived by letting each inorganic sulfur be S^{2-} (sulfide) as opposed to "actual" core oxidation state which would consider also the disulfide bridge $(S_2)^{2-}$.

II. Description of the Different Oxidation States of the P-Clusters

The P-clusters have been observed in four different oxidation states, referred to as P^N, P^{pOX} ("partially" oxidized), P^{OX}, and P^{sOX} ("super" oxidized). Table 1 summarizes the different potential oxidation states of a P-cluster and what can be inferred from the known EPR data. Let us start with the most reduced of the four states found in the native protein. In the oxidation state P^N, a distinctive spectroscopic signature of the P-cluster consists of one Mössbauer component called "Fe^{2+}" with a quadrupole splitting and an isomer shift ($\Delta E_Q = 3.02$ mm/s, $\delta = 0.69$ mm/s for Av[3] and $\Delta E_Q = 3.00$ mm/s, $\delta = 0.64$ mm/s for Cp[16]) similar to that measured for the high-spin ferrous site of rubredoxin ($\Delta E_Q = 3.27$ mm/s, $\delta = 0.71$ mm/s in *Desulfovibrio gigas*[19]). Also observed are three identical components called D with a marked ferrous character since the isomer shift δ is +0.63 mm/s on average.[5] It is thus reasonable to think of the state P^N as being all-ferrous.[5] Consequently a P-cluster in its redox state P^N can be thought of as made of two bridged "classic" $[Fe_4S_4]^0$ clusters. More precisely, a P-cluster formula can be written as $\{(Fe_4S_3)-S_2-(Fe_4S_3)\}^{n+2}(SR^{-1}_{bridge})_2(SR^{-1}_{ligand})_4(OR^{-1})$; the subunit $\{(Fe_4S_3)-S_2-(Fe_4S_3)\}^{n+2}$ emphasizes the presence of a disulfide bond $(S_2)^{2-}$ and the exponent +2 reflects the proposal (based on X-ray evidence[2]) that two inorganic sulfurs S^{2-} with total charge (−4) (as in a "classic" cluster) instead form a bridging disulfide $(S_2)^{2-}$ of total charge

(6) (a) Brink, D. M.; Satchler, G. R. *Angular Momentum*, 2nd ed.; Oxford University Press: London, 1968. (b) Edmonds, A. R. *Angular Momentum in Quantum Mechanics*; Princeton University Press: Princeton, NJ, 1957; Chapter 6 pp 90–108. (c) Wigner, E. P. *Group Theory*; Academic Press: New York, 1959; Chapter 27, pp 349–356. (d) Griffith, J. S. *Struct. Bonding (Berlin)* **1972**, *10*, 87. (e) Munck, E. *Meth. Enzymol.* **1978**, *54*, 346.
(7) Gibson, J. F.; Hall, D. O.; Thornley, J. H. M.; Whatley, F. R. *Proc. Natl. Acad. Sci. U.S.A.* **1966**, *56*, 987–990.
(8) Griffith, J. S. *Struct. Bonding (Berlin)* **1972**, *10*, 87–126.
(9) Kent, T. A.; Huynh, B. H.; Munck, E. *Proc. Natl. Acad. Sci. U.S.A.* **1980**, *77*, 6574–6576.
(10) Surerus, K. K.; Kennedy, M. C.; Beinert, H.; Munck, E. *Proc. Natl. Acad. Sci. U.S.A.* **1989**, *86*, 9846–9850.
(11) Kennedy, M. C.; Kent, T. A.; Emptage, M.; Merkle, H.; Beinert, H.; Münck, E. *J. Biol. Chem.* **1984**, *259*, 14463–14471.
(12) (a) Münck, E.; Kent, T. A. *Hyperfine Interact.* **1986**, *27*, 161–172. (b) Papaefthymiou, V.; Girerd, J.-J.; Moura, I.; Moura, J. J. G.; Münck, E. *J. Am. Chem. Soc.* **1987**, *109*, 4703–4710. (c) Münck, E.; Papaefthymiou, V.; Surerus, K. K.; Girerd, J.-J. *Metals in Proteins*; ACS Symposium Series, American Chemical Society; 1988; Chapter 15, pp 303–325.
(13) (a) Middleton, P.; Dickson, D. P. E.; Johnson, C. E.; Rush, J. D. *Eur. J. Biochem.* **1978**, *88*, 135. (b) Middleton, P.; Dickson, D. P. E.; Johnson, C. E.; Rush, J. D. *Eur. J. Biochem.* **1980**, *104*, 289.
(14) Noodleman, L. *Inorg. Chem.* **1988**, *27*, 3677–3679.
(15) (a) Noodleman, L. *Inorg. Chem.* **1991**, *30*, 246–255. (b) Noodleman, L. *Inorg. Chem.* **1991**, *30*, 256–264.
(16) Huynh, B. H.; Henzl, M. T.; Christner, J. A.; Zimmermann, R.; Orme-Johnson, W. H.; Munck, E. *Biochim. Biophys. Acta* **1980**, *623*, 124–138.
(17) Werst, M. M.; Kennedy, M. C.; Houseman, A. L. P.; Beinert, H.; Hoffman, B. M. *Biochemistry* **1990**, *29*, 10533.
(18) Rius, G.; Lamotte, B. *J. Am. Chem. Soc.*, **1989**, *111*, 2464.
(19) Moura, I.; Huynh, B. H.; Hausinger, R. P.; Le Gall, J.; Xavier, A. V.; Munck, E. *J. Biol. Chem.* **1980**, *255*, 2493–2498.

−2. This could also be written as $[Fe_4S_4]^{n_1+1}[Fe_4S_4]^{n_2+1}$ with $n = n_1 + n_2$, where n_1 and n_2 are the formal charges expected for the two "classic" cubane cores as ferredoxin or HiPIP, and n is the total charge of that system of two separated cubanes (hence $n_1 = n_2 = 0$ for the redox state P^N and $n_1 = n_2 = 1$ for the state P^{OX}). OR^{-1} represents a deprotonated serine ligand. An alternative view due to Bolin and co-workers (based on *Clostridium pasteurianum*) is that the two P-cluster halves share a sulfide corner atom which becomes therefore coordinated to six iron atoms[20,21] (another possibility along the same lines is that of a vacancy site in place of a sulfide (S^{2-}) ligand in one of the two cubanes). The counting of the charge is identical in both models, and the net charge of a P-cluster in either model is ($n - 5$). It is interesting to note that a single classic all-ferrous cubane, with its ligands, would be an anion of total charge −4. An "all ferrous" P-cluster (8Fe) however would have a total charge of −5, that is only −2.5 per "cubane" or half of the P-cluster. The "merging" of two classic cubanes into a single 8Fe P-cluster allows therefore for more reduced Fe oxidation states for comparable total charge.

Upon one-electron oxidation (from P^N to a state we call P^{pOX}) we expect to be able to observe a Kramers system. The early phase of thionin titration of *A. vinelandii* component 1 (Av1) is accompanied by the appearance of a $g = 1.94$ EPR signal.[5,22] More recently, EPR measurements performed on this oxidation state of Av (where P-clusters are expected to be in their P^{pOX} states), show signals at $g = 2.06$, 1.95, and 1.82 (average: 1.94) assigned to a spin $^1/_2$ state.[23] A value of 1.94 is comparable to typical average g values for reduced 4Fe ferredoxins, and we can consequently model the P^{pOX} state as formally a $[Fe_4S_4]^+$ cluster linked to a diamagnetic all-ferrous cubane. However, further inflections at $g = 6.67$ and 5.30 in P^{pOX} have been observed, identified as belonging to a spin $^5/_2$ state[23] (the third inflection is calculated to be at $g = 1.97$, most probably masked by the 1.95 signal of the spin $^1/_2$ species), which presumably exists as a physical mixture with the $S = {}^1/_2$ state. We will take this information into account below when we list the different spin coupling schemes possible for the state P^{OX}.

A further one-electron oxidation yields the state P^{OX}. Since magnetic hyperfine interactions were observed by Mössbauer at zero-field, it was originally thought that P^{OX} was a Kramers system.[4] Since the P^N state is diamagnetic and two electrons are required to oxidize P^N into P^{OX}, each of the P-clusters was thought to consist of 4Fe cubane-type clusters, the two cubanes being well separated. The P^{OX} state is now recognized as being a non-Kramers system of total spin $S_t = 3$ or 4,[5] consistent with the notion that the P-cluster is in fact a 8Fe cluster. It is expected therefore, since P^N is "all-ferrous", that P^{OX} is composed formally of two coupled $[Fe_4S_4]^+$ clusters. This leads, in turn, to a reanalysis of the hyperfine data available for nitrogenase, as we discuss below.

A final oxidation of P^{OX} by one electron to give P^{sOX} results in a physical mixture of spin states with $S = {}^1/_2$ and $S = {}^7/_2$.[24,25] A similar $S = {}^7/_2$ signal has been observed for the selenium substituted $2[Fe_4Se_4]^+$ clostridial ferredoxins[26,27] and hyperfine parameters as measured by Mössbauer spectroscopy are also available.[28] Such an $S = {}^7/_2$ state is easily obtained if three ferrous ions (of spin 2) ferromagnetically couple to a resultant spin $S^* = 6$. This spin can then be antiferromagnetically coupled to the remaining high-spin ferric ion (of spin $^5/_2$) to yield a net spin of $^7/_2$.[15,28] This state can be written in the slightly more general manner as follows: $|S(2Fe^{2+}), S^*, S\rangle = |4, 6, {}^7/_2\rangle$. The state of spin $^1/_2$ is reminiscent of reduced 4Fe ferredoxins, formally composed of a mixed-valence pair $Fe^{2.5+}$–$Fe^{2.5+}$ coupled to spin $^9/_2$, which is in turn antiferromagnetically coupled to a ferrous pair Fe^{2+}–Fe^{2+} of spin 4, resulting in the observed $S = {}^1/_2$. This spin-coupled state is therefore written as follows: $|S(Fe^{2.5+}–Fe^{2.5+}), S(Fe^{2+}–Fe^{2+}), S\rangle = |{}^9/_2, 4, {}^1/_2\rangle$.

Two views are possible regarding the description of the spin distribution in a P-cluster.[23,29] The spin density may be delocalized over the whole 8Fe cluster, or may reside largely on half (4Fe) of the cluster for some oxidation states like P^{pOX} and P^{sOX}. In that second view, when both halves of the cluster become paramagnetic, spin-coupling interactions occur, resulting in a global coupled state. Within this model, the spin $^7/_2$ observed for the redox state P^{sOX} could be associated with only half of the P-cluster. From the X-ray structure[2] (for the native protein, that is with the P-cluster in the redox state P^N), the halves of the P-cluster are not equivalent as far as the immediate coordination environment is concerned, and there are also inequivalences in the longer range protein environment. One of the irons is observed to be close to the serine residue 188 in Av1 which may be able to coordinate this iron site (see Figure 1). This has important consequences at the level of the geometry of the whole cluster which we discuss now on the basis of the 2.2 Å resolution structure of Av.[2,30] Cubane 1 (on the left in Figure 1) looks very much like a "standard" 4Fe cubane: the average Fe–Fe distance is of 2.86 Å (against 2.74 Å for the ferredoxins), with a distribution of ±5% around that value (minimum 2.73 Å and maximum 2.99 Å). The other half however (cubane 2, closest to the serine) presents a clear distortion, related to the presence of that extra coordination for one of the irons. Two of the six Fe–Fe distances are very large: 3.42 and 3.25 Å, involving the iron coordinated to the serine and the two irons facing cubane 1 (coordinated to the bridged cysteines). The four other Fe–Fe distances average to 2.89 Å, close to that average value obtained for cubane 1 (2.86 Å). Apparently, the pentacoordinated iron is pulled toward the serine residue, distinguishing it from the three others belonging to cubane 2 (and from the irons of cubane 1). The two Fe–Fe distances between the irons coordinated to the same bridging cysteine (one iron of each cubane) average to 3.08 Å. It can be expected that the presence of this serine ligand may induce a state of spin $^7/_2$ (trapped valence situation with one ferric and three ferrous ions) rather than a state of spin $^1/_2$ (partial delocalization over a mixed-valence pair) as in "classic" 4Fe

(20) Bolin, J. T.; Ronco, A. E.; Mortenson, L. E.; Morgan, T. V.; Williamson, M.; Xuong, N.-H. In *Nitrogen Fixation: Achievements and Objectives. Proceedings of the 8th International Congress on Nitrogen Fixation*; Grashoff, P. M., Roth, L. E., Stacey, G., Newton, W. E., Ed., Chapman and Hall: New York, 1990; 117–124.
(21) Bolin, J. T.; Campobasso, N.; Muchmore, S. W.; Morgan, T. V.; Mortenson, L. E. In *Molybdenum Enzynme, Cofactors and Models*; Stiefel, E.; Coucouvanis, D., Newton, W. E., Eds.; American Chemical Society: Washington, DC., 1993; Chapter 12, pp 187–195.
(22) Orme-Johnson, W. H.; Orme-Johnson, N. R.; Touton, C.; Emptage, M.; Henzl, M.; Rawlings, J.; Jacobson, K.; Smith, J. P.; Mims, W. B.; Huynh, B. H.; Jacob, G. S. In *Molybdenum Chemistry of Biological Significance*; Newton, W. E., Otsuka, S.; Eds.; Plenum Press: New York, London, 1980; pp 85–94.
(23) Tittsworth, R. C.; Hales, B. J. *J. Am. Chem. Soc.* **1993**, *115*, 9763–9767.
(24) Hagen, W. R.; Wassink, H.; Eady, R. R.; Smith, B. E.; Haaker, H. *Eur. J. Biochem.* **1987**, *169*, 457–465.
(25) Pierik, A. J.; Wassink, H.; Haaker, H.; Hagen, W. R. *Eur. J. Biochem.* **1993**, *212*, 51–61.
(26) Moulis, J.-M.; Auric, P.; Gaillard, J.; Meyer, J. *J. Biol. Chem.* **1984**, *259*, 11396–11401.
(27) Gaillard, J.; Moulis, J.-M.; Auric, P.; Meyer, J. *Biochemistry* **1986**, *25*, 464–468.
(28) Auric, P.; Gaillard, J.; Meyer, J.; Moulis, J.-M. *Biochem. J.* **1987**, *242*, 525–530
(29) Oliver, M. E.; Hales, B. J. *J. Am. Chem. Soc.* **1992**, *114*, 10618–10623.
(30) Rees, D. C. Private communication.

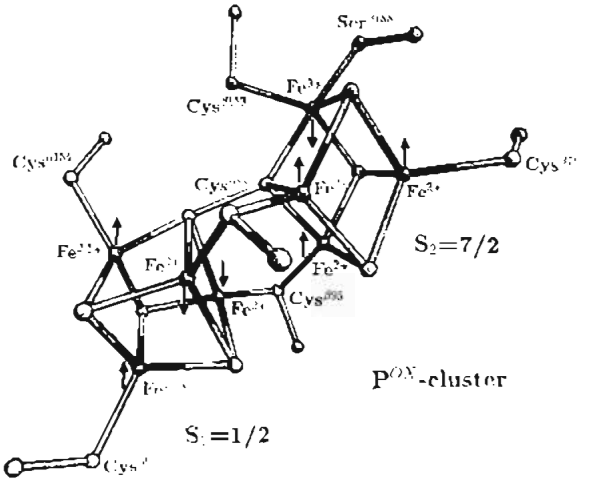

Figure 1. Schematic representation of the P-cluster model of ref 2 in its native state. The oxidation states of the iron ions are for the redox state P^{OX} and are located according to Section IV. Cubane 1 (left, with spin $S_1 = {}^1/_2$) and cubane 2 (right, with spin $S_2 = {}^7/_2$) are represented, according to the conclusion of our model. The arrows indicate if the local monomer spin of the iron is in the same or opposite direction to the total spin $S_t = 4$ of the whole cluster.

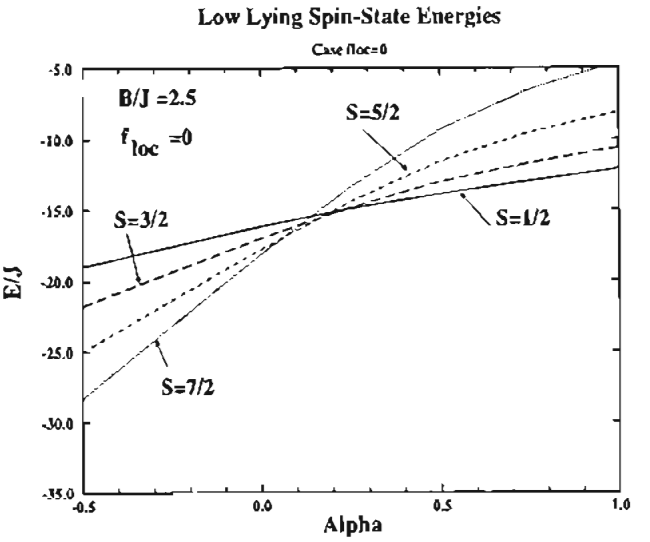

Figure 2. Plots of the low-lying energy states of $[Fe_4S_4]^{1+}$ for $S = {}^1/_2$, ${}^3/_2$, ${}^5/_2$, and ${}^7/_2$. The ratio B/J is 2.5 and the states are delocalized ($f_{loc} = 0$; that is the mixed-valence pair is delocalized).

ferredoxins, especially if this serine is deprotonated. We would expect therefore the ferric ion to be localized on the site closest to the serine. The other half of the cluster is, in this scheme, diamagnetic (and therefore EPR-silent) in P^{sOX} and is analogous to an oxidized 4Fe ferredoxin composed of four equivalent formal $Fe^{2.5+}$. The $S = {}^1/_2$ signal also observed for P^{sOX} would then correspond to the oxidation of the other half of the cluster, the cubane closest to the serine now becoming diamagnetic. From now on, we will distinguish the halves of the P-cluster by calling S_1 the spin of cubane 1 without the adjacent serine (for which we expect the values 0 or ${}^1/_2$) and S_2 the spin of cubane 2 (with values of ${}^5/_2$ or ${}^7/_2$ when this half is paramagnetic and 0 when diamagnetic).

The discussion above is based on the X-ray structure of Av nitrogenase by Rees and co-workers.[1,2] Again, there are some differences here with the structure of Cp by Bolin and co-workers.[21] Bolin finds that the serine oxygen is further away from the closest Fe at 3.2 Å, so that a hydrogen bond to a cluster S instead of a direct Fe−O bond is implicated. These longer range asymmetries could still be sufficient to stabilize an $S = {}^7/_2$ trapped valence cubane, although the structural relationship is less strong than that for the Av structure. At present, it is not possible to remove all ambiguities and contradictions between the Bolin and Rees X-ray structures. Both structures are for the P^N state; there can be differences between Av1 and Cp1, and there may also be structural differences between P^N and P^{OX}. For example, it is possible that there is direct serine coordination for both P^N and P^{OX} for Av1, but that this occurs only for P^{OX} and not for P^N in Cp1. This would rationalize the very similar Mössbauer spectra of Av1 and Cp1 for P^{OX},[4,16] while allowing for structural differences between Av1 and Cp1 for P^N. Final resolution of these issues awaits further X-ray structural and Mössbauer studies. For the present, we take the working hypothesis that cubane 2 with the adjacent serine has a more asymmetric environment than cubane 1.

In the spin coupling analysis to follow, we have assumed that the coupling between cubanes is weak compared to that within each cubane (i.e., compared to the energy separation of the lowest spin multiplets in each), so that only the ground spin states of the individual cubanes need to be considered in the coupling problem. This vastly simplifies the coupling problem and also has a good structural basis.[1,2,21] Each Fe on the cube face adjacent to the bridging cysteine has only one Fe near neighbor on the opposite cube (average distance 3.08 Å). The distance to the other Fe on the opposite cube face is considerably larger. It is then expected that spin interactions of Fe sites is greater within a cube where there are four (cubane 2) or six (cubane 1) near neighbor Fe−Fe distances < 3.0 Å, compared with interactions between cubanes where there are only two Fe−Fe distances at 3.08 Å and two other much further apart. Finally, bridging cysteine is probably not as effective in mediating exchange coupling (nor is a bridging disulfide, nor a six-coordinate sulfide, nor a sulfide plus a vacancy site) compared with sulfides within a cubane. Similar considerations apply to both the Av and Cp structures in this respect, so that using the ground state cubane spin quantum numbers in composing the total spin should be a good procedure.

III. Spin Coupling Analysis for P^{OX}

From the experimental evidence presented at the end of the last section, it is natural to consider that, upon reduction of P^{sOX} into P^{OX}, the $S_2 = {}^7/_2$ half of the P-cluster is conserved while the other half is effectively reduced from $[Fe_4S_4]^{2+}$ ($S_1 = 0$) to $[Fe_4S_4]^{+}$ ($S_1 = {}^1/_2$). This scheme yields a total spin S_t for P^{OX} of 3 (if spins ${}^1/_2$ and ${}^7/_2$ are antiferromagnetically coupled) or 4 (if the same spins are ferromagnetically coupled). As an alternative model, we cannot eliminate the possibility of a spin ${}^1/_2$ and a spin ${}^5/_2$ coupled to 3 (since both spins ${}^1/_2$ and ${}^5/_2$ have been observed in P^{pOX}). This state of spin $S_2 = {}^5/_2$ is analogous to that of spin $S_2 = {}^7/_2$ and is written as: $|S(2Fe^{2+}) = 4, S^* = 5, S_2 = {}^5/_2\rangle$. However, a recent theoretical model aimed at describing the different spin states possible for $[Fe_4S_4]^{+}$ clusters showed that the ground states with $S_1 = {}^1/_2$ or $S_2 = {}^7/_2$ are the most likely.[15] This study considered a spin Hamiltonian that included Heisenberg couplings between the irons along with a resonance delocalization term for one mixed-valence pair. We show in Figures 2 and 3 the energies of low-lying spin states as a function of the parameter $\alpha = J(Fe^{2+}-Fe^{2+})/J(Fe^{2+}-Fe^{3+})$, the ratio of the Heisenberg coupling parameters for a pair of ferrous sites to that for a mixed-valence (ferric-ferrous) pair. B/J is the ratio of the resonance delocalization parameter to $J(Fe^{2+}-Fe^{3+})$, and $f_{loc} = E_{loc}/B$ represents the site stabilization energy[15] (scaled by B), describing the localization of the extra electron of the mixed-valence pair $Fe^{2.5+}-Fe^{2.5+}$ ($f_{loc} = 0$) to one of the two sites yielding $Fe^{2+}-Fe^{3+}$ ($f_{loc} > 0$). The energy

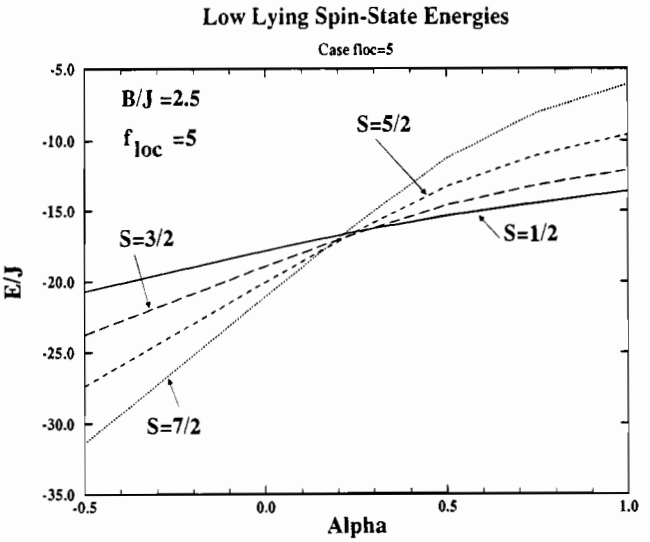

Figure 3. Plots of the low-lying energy states of $[Fe_4S_4]^{1+}$ for $S = {}^1/_2$, ${}^3/_2$, ${}^5/_2$, and ${}^7/_2$. The ratio B/J is the same as in Figure 2, but the states are partially localized ($f_{loc} = 5$; that is the extra electron of the mixed-valence pair is localized to a particular site).

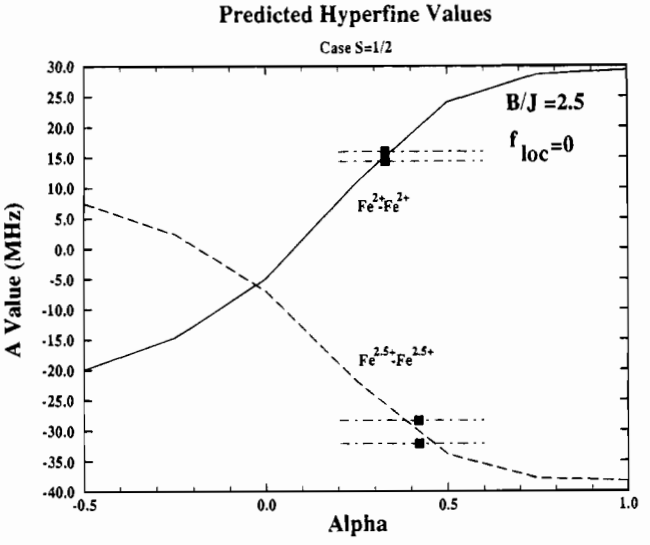

Figure 4. Predicted theoretical hyperfine values for the ferrous pair Fe^{2+}–Fe^{2+} (solid line) and the mixed-valence pair $Fe^{2.5+}$–$Fe^{2.5+}$ (dashed line) in the case $S = {}^1/_2$ ($f_{loc} = 0$). The corresponding experimental values are represented by the filled squares (from Table 2).

E_{loc} would be typically, for a stabilization due to the protein environment, on the order of a few kilocalories per mole (corresponding to $0 < f_{loc} < 5$ for example).[15]

As an illustration, we show results of this model for different values of the parameter f_{loc} in Figure 2 ($f_{loc} = 0$) and Figure 3 ($f_{loc} = 5$) to reflect the two different physical situations (delocalization of the electron over the mixed-valence pair, $S = {}^1/_2$, or localization of that same electron, $S = {}^7/_2$). As can be seen from a comparison of the two figures, the effect of increasing the value of f_{loc} is that while the overall pattern of the $S = {}^1/_2$, ${}^3/_2$, ${}^5/_2$, and ${}^7/_2$ energy curves are similar, the parameter range of α for which the $S = {}^7/_2$ state is the ground state is shifted toward larger values of α (from $\alpha < 0.05$ for $f_{loc} = 0$ to $\alpha < 0.15$ for $f_{loc} = 5$) making that state more likely to occur. It can be also seen that the span in parameter space for which the states $S_2 = {}^3/_2$ and $S_2 = {}^5/_2$ become the ground state is very small (roughly $0.1 < \alpha < 0.2$).

We present also in Figures 4 and 5 the predicted hyperfine values for the states $S = {}^1/_2$ and $S = {}^7/_2$, as a function of α. Comparison with experimental cubane hyperfine parameters as

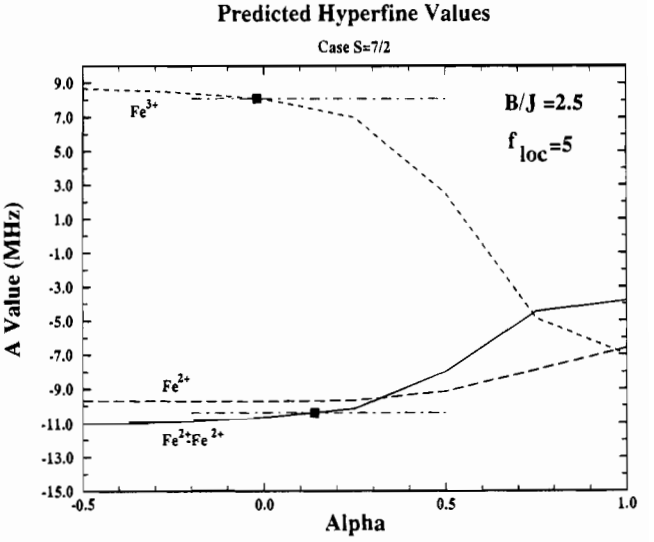

Figure 5. Predicted theoretical hyperfine values for the ferrous pair Fe^{2+}–Fe^{2+} (solid line) and the mixed-valence pair Fe^{2+}–Fe^{3+} (dashed lines) in the case $S = {}^7/_2$ ($f_{loc} = 5$). The corresponding experimental values are represented by the filled squares (from Table 2).

found in Table 2 allows us to determine, within our theoretical model, the range of α that is compatible with experiment. In the case $S = {}^1/_2$, α is found within the range [0.3–0.5], a range for which the ground state predicted in Figure 2 is $S = {}^1/_2$. For $S = {}^7/_2$, the range of parameter space where there is agreement between theory and experiment for hyperfine parameters is $\alpha < 0.3$. For most of that range ($\alpha < 0.2$), the correct ground spin state with $S = {}^7/_2$ is anticipated from Figure 3. Therefore within each of the two intervals of α we defined from the hyperfine values for the cases $S = {}^1/_2$ and $S = {}^7/_2$, the correct ground spin state is predicted.

Finally, we consider also the possibility of coupling of a spin $S_1 = {}^3/_2$ to a spin $S_2 = {}^5/_2$ or ${}^7/_2$. It is known that reduced 4Fe ferredoxins can appear with a spin ${}^3/_2$ ground state, both in protein systems (e.g. the $[Fe_4Se_4]^+$ clusters in selenium-reconstituted clostridial ferredoxins[26] or the $[Fe_4S_4]^+$ in the Fe protein of Av2 nitrogenase[31]) and more frequently for synthetic analogues (as a spin-mixture of ${}^1/_2$ and ${}^3/_2$: see ref 32 and references therein for examples). We can see from Table 2 that, whenever a spin ${}^3/_2$ is observed for a reduced 4Fe ferredoxins, the four hyperfine coupling constants observed are all negative. This situation can best be described by the state $|S(2Fe^{2+}) = 4, S^* = 2, S_1 = {}^3/_2\rangle$.[15] We will therefore consider three additional states that might be associated with P^{OX}: $|{}^3/_2, {}^7/_2, 3\rangle$, $|{}^3/_2, {}^7/_2, 4\rangle$ and $|{}^3/_2, {}^5/_2, 4\rangle$ and carry out, for the sake of completeness, the spin algebra for the six following spin states:

$$\left\{\begin{array}{l} |{}^1/_2, {}^7/_2, 3\rangle \\ |{}^1/_2, {}^7/_2, 4\rangle \\ |{}^1/_2, {}^5/_2, 3\rangle \\ |{}^3/_2, {}^7/_2, 3\rangle \\ |{}^3/_2, {}^7/_2, 4\rangle \\ |{}^3/_2, {}^5/_2, 4\rangle \end{array}\right. \quad (6)$$

The second, third, and last states evidently imply a *ferromagnetic* coupling between the two spins S_1 and S_2 (since $S_1 +$

(31) Lindahl, P. A.; Day, E. P.; Kent, T. A.; Orme-Johnson, W. H.; Münck, E. *J. Biol. Chem.* **1985**, *260*, 11160.
(32) Carney, M. J.; Papaefthymiou, G. C.; Spartalian, K.; Frankel, R. B.; Holm, R. H. *J. Am. Chem. Soc.* **1988**, *110*, 6084–6095.

Table 2. Hyperfine Parameters for $[Fe_4X_4]^+$ Clusters[a]

system	$A(Fe^{3+})$	$A(Fe^{2.5+})$	$A(Fe^{2+})$	a_{test}[b]	ref
		$[Fe_4X_4]^+$ ($S = {}^1/_2$)			
Av2 protein		−29.7 (×2)	+15.7 (×2)	−28.0	31
B. stearothermophilus Fd		−30.3 (×2)	+16.0 (×2)	−28.6	13a,31
$[Fe_4S_4(S\text{-}p\text{-}C_6H_4Br)_4]^{3-}$		−31.8 (×2)	+15.1 (×2)	−32.4	32
$2[Fe_4S_4(SR)_4]^{3-}$ Cp Fd		−28.3 (×2)	+14.4 (×2)	−27.8	34
$2[Fe_4Se_4(SR)_4]^{3-}$ Cp Fd		−32.1 (×2)	+15.3 (×2)	−33.6	28
av. $A_{av}(Fe_i)$		−30.4 (×2)	+15.3 (×2)	−30.2	
aconitase		b_2: −36	a: +29		17
(substrate bound)		b_3: −40	b_1: +15		
av. $A_{av}(Fe_i)$		−38 (×2)	+22	−32	
		$[Fe_4X_4]^+$ ($S = {}^3/_2$)			
Av2/urea		−7.8 (×2)	−4.1 (×2)	−23.8	31
$[Fe_4S_4(SC_6H_{11})_4]^{3-}$		−8.9 (×2)	−8.9 (×2)	−35.6	32
$2[Fe_4Se_4(SR)_4]^{3-}$ Cp Fd		−3.8 (×2)	−3.8 (×2)	−15.2	28
av. $A_{av}(Fe_i)$		−6.8 (×2)	−5.6 (×2)	−24.9	
		$[Fe_4Se_4]^+$ ($S = {}^7/_2$)			
$2[Fe_4Se_4(SR)_4]^{3-}$ Cp Fd	+8.1 (×1)		−10.4 (×3)	−23.1	28

[a] Values in MHz for various cubane clusters in the +1 core oxidation state; "(×2)" implies that two components were observed with nearly (or exactly) the same value (similarly for "(×3)" and "(×1)"). [b] Calculated from eq 7.

$S_2 = S_t$) whereas the first one describes a situation of *antiferromagnetism* ($S_2 - S_1 = S_t$). The two remaining states have intermediate couplings. We will see below that analysis of hyperfine couplings allows us to decide which of these couplings is the most likely.

A summary of our analysis of the oxidation and spin states of the P-clusters is presented in Table 1. In this model, the site of oxidation (or reduction) alternates between the two halves of the P-cluster upon removing (or adding) one electron. We consider next the state P^{OX} for which Mössbauer measurements of the hyperfine coupling constants have been done.

IV. Hyperfine Coupling Constants of P^{OX}

Two MoFe proteins have been studied by Mössbauer spectroscopy, one from *A. vinelandii*[4], the other from *C. pasteurianum*.[16] In both cases, eight values of internal magnetic fields are reported, given by $H^i_{int} = +S_t A_{iz}/g_n\beta_n$ with S_t the spin of the cluster and A_{iz} the z-component of the hyperfine coupling tensor, where z is the ZFS axis. Four positive and four negative couplings were originally found for Av,[4] although a quite reasonable fit was also obtained if only two components were assumed to have $A_{iz} > 0$.[4] In fact, in light of a similar experimental study for Cp,[16] a reinvestigation of the data for Av led the authors to adopt this 6:2 pattern[16] (six negative and two positive, as found in Cp) and a subsequent repartitioning of four components (3, 4, 7, and 8) leading to a modification of the internal field values for these components in Av. In effect, the Mössbauer spectra of Cp and Av MoFe proteins differ only in the parameters of one component[4,16] (component 2: $H_{int} = -221$ kG in Cp but −237 kG in Av). We have collected these values in Table 3, along with the corresponding quadrupole splittings and isomer shifts. Since the values of the internal fields of both Av and Cp are so similar, we will from now on only consider the data measured for Cp and apply the conclusions we obtain from that analysis to the P-clusters of Av.

It is interesting to discuss the assumptions made by the authors of both papers to obtain their experimental fits. In the case of Av,[4] it was *assumed* that four components had a positive hyperfine coupling constant. Because of an equally good fit to the data obtained for a 6:2 pattern, the parameter set obtained for Av was not considered to be unique.[4] Note that patterns with even integers (as 6:2 or 4:4) were dictated by the fact that a P-cluster was thought to contain four irons rather than eight. In the redox state P^N, only four signals are observed (one "Fe^{2+}"

Table 3. Observed Mössbauer Parameters for Nitrogenase P-clusters

	C. pasteurianum[a]		
component	H_{int} (kG)	ΔE_Q (mm/s)	δ (mm/s)
1	−287	−1.40	+0.56
2	−221[b]	+1.53	+0.64
3	−245	+0.57	+0.40
4	−151	+0.60	+0.25
5	−259	+1.26	+0.48
6	−237	−0.72	+0.49
7	+201	+3.20	+0.65
8	+223	+2.30	+0.68

[a] Taken from ref 16. [b] This component has the value −237 kG for *A. vinelandii* (see ref 16); other values are the same for Av and Cp.

and three D but see refs 3 and 33 for further refinements), leading the authors to the assumption (since P^N is diamagnetic, whereas P^{OX} was known to be paramagnetic) that the native protein contains four spectroscopically identical 4Fe P-clusters. Upon a four-electron oxidation, these 4Fe clusters appeared in slightly inequivalent pairs (in accord with the presence of a 2-fold symmetry in the $\alpha_2\beta_2$ subunit structure of the MoFe protein). These considerations in turn can generate only such patterns for the signs of hyperfine couplings as 8:0, 6:2, 4:4, 2:6, and 0:8. With a P-cluster now known to contain eight irons, all combinations are possible a priori, including the 7:1 and 5:3 patterns.

We now have two ways to estimate hyperfine parameter values for P^{OX}. First, Mössbauer hyperfine coupling constants have been measured for reduced 4Fe ferredoxins with spin ${}^1/_2$ (ferredoxins[28,31,32,34] and aconitase[17]), spin ${}^3/_2$,[31,32] and spin ${}^7/_2$ (selenium-substituted[28]). These measured values are listed in Table 2. We can use the individual cubane hyperfine parameters of Table 2 in conjunction with the spin projection coefficients for coupling the cubane spins onto the total system spin $|S_1, S_2, S_t\rangle$ to obtain an estimate of the hyperfine coupling constants for the whole P-cluster in its P^{OX} oxidation state. The results of this approach are presented in Table 4. We note immediately that the two states $|{}^3/_2, {}^7/_2, 3\rangle$ and $|{}^3/_2, {}^7/_2, 4\rangle$ can, from now on, be discarded: the first has no spin density whatsoever associated with cubane 1 (and therefore four hyperfine couplings constants

(33) McLean, P. A.; Papaefthymiou, V.; Orme-Johnson, W. H.; Münck, E. *J. Biol. Chem.* **1987**, *262*, 12900−12903.
(34) Thomson, C. L.; Johnson, C. E.; Dickson, D. P. E.; Cammack, R.; Hall, D. O.; Weser, U.; Rao, K. K. *Biochem. J.* **1974**, *139*, 97−103.

Table 4. Predicted Hyperfine Parameters for P^{ox}

state $\|S_1, S_2, S_t\rangle$		cubane 1		cubane 2		a_{test}[a]
		$Fe^{2.5+}$ (×2)	Fe^{2+} (×2)	Fe^{3+} (×1)	Fe^{2+} (×3)	
$\|1/2, 7/2, 3\rangle$	K^q	$-1/8$	$-1/8$	$+9/8$	$+9/8$	
	$A_{av}(Fe_i)$[b]	−30.1 (−38.0)[c]	+15.3 (+22.0)[c]	+8.1	−10.4	
	A(calc)[d]	+3.8 (+4.8)	−1.9 (−2.9)	+9.1	−11.7	−22.2
$\|1/2, 7/2, 4\rangle$	K^q	$+1/8$	$+1/8$	$+7/8$	$+7/8$	
	$A_{av}(Fe_i)$[b]	−30.1 (−38.0)[c]	+15.3 (+22.0)[c]	+8.1	−10.4	
	A(calc)[d]	−3.8 (−4.8)	+1.9 (+2.9)	+7.1	−9.1	−24.0
$\|1/2, 5/2, 3\rangle$	K^q	$+1/6$	$+1/6$	$+5/6$	$+5/6$	
	$A_{av}(Fe_i)$[b]	−30.1 (−38.0)[c]	+15.3 (+22.0)[c]	*e*	*e*	
	A(calc)[d]	−5.0 (−6.3)	+2.6 (+3.7)	*e*	*e*	*e*
$\|3/2, 7/2, 3\rangle$	K^q	0	0	1	1	
	$A_{av}(Fe_i)$[b]	−6.8	−5.6	+8.1	−10.4	
	A(calc)[d]	+0.0	+0.0	+8.1	−10.4	−23.1
$\|3/2, 7/2, 4\rangle$	K^q	$+1/5$	$+1/5$	$+4/5$	$+4/5$	
	$A_{av}(Fe_i)$[b]	−6.8	−5.6	+8.1	−10.4	
	A(calc)[d]	−1.4	−1.1	+6.5	−8.3	−23.5
$\|3/2, 5/2, 4\rangle$	K^q	$+3/8$	$+3/8$	$+5/8$	$+5/8$	
	$A_{av}(Fe_i)$[b]	−6.8	−5.6	*e*	*e*	
	A(calc)[d]	−2.6	−2.1	*e*	*e*	*e*

[a] Computed from eq 7. [b] $A_{av}(Fe_i)$ values taken from Table 2. [c] Values in parentheses for aconitase. [d] $A(\text{calc}) = K^q \cdot A_{av}(Fe_i)$. [e] No experimental values available for a cubane with spin $5/2$.

would have been expected rather than eight as observed experimentally for both Av and Cp) whereas the second yields a 7:1 pattern for the hyperfine parameters (seven negative and one positive) contradicting the experimental observation of the presence of at least two positive hyperfine parameters.

As a second approach we can calculate hyperfine parameters by using spin projection coefficients in conjunction with so-called "site" or "intrinsic" values $a(Fe_i)$ corresponding to uncoupled monomers. One common set of site values found in the literature is $a(Fe^{2+}) = -22$ MHz and $a(Fe^{3+}) = -20$ MHz.[35] We have recently made an extensive study of measured hyperfine parameters for 1Fe, 2Fe, 3Fe, and 4Fe systems in different oxidation states to obtain improved intrinsic site values $a(Fe_i)$ and a better understanding of spin coupling schemes.[36] The site values $a(Fe_i)$ obtained from our study differ somewhat from the one just quoted above (we found for $S_1 = 1/2$ that $a(Fe^{2.5+}) = -22$ MHz and $a(Fe^{2+}) = -18$ MHz and for $S_2 = 7/2$ that $a(Fe^{2+}) = -22$ MHz and $a(Fe^{3+}) = -20$ MHz). These differences are not critical for our present purpose, and we will use therefore $a(Fe^{2+}) = -22$ MHz, $a(Fe^{3+}) = -20$ MHz, and $a(Fe^{2.5+}) = -21$ MHz throughout. The calculation of the spin projection coefficients is done in two steps. In a first step, for the cubane of net spin $S_1 = 1/2$, a pairwise scheme is considered, yielding spin $9/2$ for the mixed-valence pair and 4 for the ferrous pair. These dimer spins are then coupled to $1/2$, resulting in spin projection coefficients $\{K_i^1\text{'s}\}$ with i running over the four sites of this cubane, cubane 1. In the case $S > 1/2$ ($S_1 = 3/2$ for cubane 1 and $S_2 = 5/2$ or $7/2$ for cubane 2), the three ferrous ions are coupled to S^* to 2, 5, or 6, respectively. S^* is then antiferromagnetically coupled to the remaining spin $5/2$ of the ferric ion resulting in $S_q = 3/2$, $5/2$, or $7/2$. The second step leads to a coupling of the spins S_1 and S_2 of the two cubanes to the possible final state $|S_1, S_2, S_t\rangle$ with a corresponding coefficient: K^q. Each of the sets of coefficients associated with the two separate cubanes ($\{K_i^q\}$) is multiplied by the corresponding spin projection coefficient (K^q) as shown in eq 5. The intermediate ($\{K_i^q\}$, $\{K^q\}$) and final $\{K_i\}$ spin projection coefficients are given in Tables 4 and 5. The calculated hyperfine parameters $A(\text{calc}) = K_i a(Fe_i)$ are also presented in Table 5.

Tables 4 and 5 lead to rather similar conclusions. As already noted, the states $|3/2, 7/2, 3\rangle$ and $|3/2, 7/2, 4\rangle$ can be discarded. The $|3/2, 5/2, 4\rangle$ state also results in a 7:1 pattern for the hyperfine parameters, and so can be discarded. We also note that the two different procedures (shown in Tables 4 and 5) described above yield similar calculated hyperfine parameters (apart from some minor differences in magnitude). This consistency further justifies the use of site values for the estimation of the hyperfine parameters of the state $|1/2, 5/2, 3\rangle$. Together with $|1/2, 7/2, 4\rangle$ and $|1/2, 7/2, 3\rangle$, these three states result in five negative and three positive hyperfine coupling constants rather than in a 4:4 or 6:2 pattern. We also note that the hyperfine parameters calculated for the $S_2 = 5/2$ or $7/2$ halves tend to be greater in magnitude than those of the $S_1 = 1/2$ half, as a result of the fact that the spin projection coefficients K^2 associated with coupling the spin S_2 onto total spin S_t are larger than the corresponding spin projection coefficients K^1 (see Table 4). This in turn will result in larger observed hyperfine coupling constants predicted for the iron atoms associated with cubane 2.

Let us reexamine the information in Table 3. The components labeled 7 and 8 definitely have a positive internal field (and positive hyperfine couplings). Moreover, their isomer shifts are clearly indicative of a marked ferrous character: +0.65 and +0.68 mm/s for Cp. A second common feature concerns the components 1 and 2. The isomer shifts (+0.64 mm/s for component 2, and +0.56 mm/s for component 1) are again indicative of ferrous character, and the associated hyperfine coupling constants are negative (the measured quadrupole splittings further support these assignments). These two observations allow us to predict that the mode of coupling of the two spins S_1 and S_2 of the two cubanes (within the working hypothesis of having $S_1 = 1/2$ and $S_2 = 5/2$ or $7/2$) must be ferromagnetic. In effect within cubane 1, the spin $S(Fe^{2+}-Fe^{2+})$ of the ferrous pair is aligned oppositely to spin S_1, whereas in cubane 2, the spin S^* of the three ferrous ions is parallel to S_2. Only a ferromagnetic coupling of the two spins S_1 and S_2 of the cubanes can be compatible with the experimental observations cited just above. This result can also be seen in Table 4: coupling the two spins S_1 and S_2 antiferromagnetically ($S_t = 3$) results in negative hyperfine coupling constants for *all* the ferrous ions. We can thus eliminate the state $|1/2, 7/2, 3\rangle$, which contains antiferromagnetism between the two cubanes. This allows us to identify components 1 and 2 with two of the three ferrous ions of the $S_2 = 7/2$ (or $5/2$) cubane and components

(35) Papaefthymiou, V.; Girerd, J.-J.; Moura, I.; Moura, J. J. G.; Munck, E. *J. Am. Chem. Soc.* **1987**, *109*, 4703.
(36) Mouesca, J.-M.; Noodleman, L.; Case, D. A.; Lamotte, B. Submitted for publication.

Table 5. Spin Projection Coefficients and Hyperfine Parameters Using Site Values $a(Fe_i)$[a]

state $\|S_1, S_2, S_t\rangle$		cubane 1 substate	cubane 1 $Fe^{2.5+}$ (×2)	cubane 1 Fe^{2+} (×2)	cubane 2 substate	cubane 2 Fe^{3+} (×1)	cubane 2 Fe^{2+} (×3)	a_{test}
	K_i^q	$\|^9/_2, 4, {}^1/_2\rangle$[c]	$+^{11}/_6$	$-^4/_3$	$\|4, 6, {}^7/_2\rangle$[d]	$-^5/_9$	$+^{14}/_{27}$	
$\|^1/_2, {}^7/_2, 3\rangle$[b]	$K_i = K^q K_i^q$		$-^{11}/_{48}$	$+^1/_6$		$-^5/_8$	$+^7/_{12}$	
	A(calc)[e]		+4.8	−3.7		+12.5	−12.8	−23.7
	K_i^q	$\|^9/_2, 4, {}^1/_2\rangle$[c]	$+^{11}/_6$	$-^4/_3$	$\|4, 6, {}^7/_2\rangle$[d]	$-^5/_9$	$+^{14}/_{27}$	
$\|^1/_2, {}^7/_2, 4\rangle$[b]	$K_i = K^q K_i^q$		$+^{11}/_{48}$	$-^1/_6$		$-^{35}/_{72}$	$+^{49}/_{108}$	
	A(calc)[e]		−4.8	+3.7		+9.9	−10.0	−22.3
	K_i^q	$\|^9/_2, 4, {}^1/_2\rangle$[c]	$+^{11}/_6$	$-^4/_3$	$\|4, 5, {}^5/_2\rangle$[d]	$-^5/_7$	$+^4/_7$	
$\|^1/_2, {}^5/_2, 3\rangle$[b]	$K_i = K^q K_i^q$		$+^{11}/_{36}$	$-^2/_9$		$-^{25}/_{42}$	$+^{20}/_{42}$	
	A(calc)[e]		−6.4	+4.9		+11.9	−10.5	−22.6
	K_i^q	$\|4, 2, {}^3/_2\rangle$[d]	$+^7/_{18}$	$+^1/_9$	$\|4, 6, {}^7/_2\rangle$[d]	$-^5/_9$	$+^{14}/_{27}$	
$\|^3/_2, {}^7/_2, 3\rangle$[b]	$K_i = K^q K_i^q$		0	0		$-^5/_9$	$+^{14}/_{27}$	
	A(calc)[e]		+0.0	+0.0		+11.1	−11.4	−23.1
	K_i^q	$\|4, 2, {}^3/_2\rangle$[d]	$+^7/_{18}$	$+^1/_9$	$\|4, 6, {}^7/_2\rangle$[d]	$-^5/_9$	$+^{14}/_{27}$	
$\|^3/_2, {}^7/_2, 4\rangle$[b]	$K_i = K^q K_i^q$		$+^7/_{90}$	$+^1/_{45}$		$-^4/_9$	$+^{56}/_{135}$	
	A(calc)[e]		−1.6	−0.5		+8.9	−9.1	−22.6
	K_i^q	$\|4, 2, {}^3/_2\rangle$[d]	$+^7/_{18}$	$+^1/_9$	$\|4, 5, {}^5/_2\rangle$[d]	$-^5/_7$	$+^4/_7$	
$\|^3/_2, {}^5/_2, 4\rangle$[b]	$K_i = K^q K_i^q$		$+^7/_{48}$	$+^1/_{24}$		$-^{25}/_{56}$	$+^{20}/_{56}$	
	A(calc)[e]		−3.1	−0.9		+8.9	−7.9	−22.8

[a] $a(Fe^{3+}) = -20$ MHz, $a(Fe^{2.5+}) = -21$ MHz and $a(Fe^{2+}) = -22$ MHz. [b] State $|S_1,S_2,S_t\rangle$. [c] State $|S(2Fe^{2.5+}),S(2Fe^{2+}),S_1\rangle$. [d] State $|S(2Fe^{2+}),S^*,S_2\rangle$. [e] $A(\text{calc}) = K_i a(Fe_i)$; in the expression of $K_i = K^q K_i^q$, the values of K^q are reported from Table IV.

Table 6. Comparison Theory/Experiment for $S_t = 3$

component	exptl A_{iz} Cp (for $S_t = 3$)	theor A(calc) $\|^1/_2, {}^5/_2, 3\rangle$	assignt
1	−13.2	−10.5	Fe^{2+} (S_2)
2	−10.1[a]	−10.5	Fe^{2+} (S_2)
3	−11.2	−6.4	$Fe^{2.5+}$ (S_1)
4	(+6.9)[b]	+11.9	Fe^{3+} (S_2)
5	−11.9	−10.5	Fe^{2+} (S_2)
6	−10.9	−6.4	$Fe^{2.5+}$ (S_1)
7	+9.2	+4.9	Fe^{2+} (S_1)
8	+10.2	+4.9	Fe^{2+} (S_1)

[a] This component has the value −10.8 MHz for Av. [b] Hyperfine coupling from ref 16 for which the sign as been changed.

Table 7. Comparison Theory/Experiment for $S_t = 4$

component	exptl A_{iz} Cp (for $S_t = 4$)	theor A(calc) $\|^1/_2, {}^7/_2, 4\rangle$	assignt
1	−9.9	−10.0	Fe^{2+} (S_2)
2	−7.6[a]	−10.0	Fe^{2+} (S_2)
3	−8.4	−4.8	$Fe^{2.5+}$ (S_1)
4	(+5.2)[b]	+9.9	Fe^{3+} (S_2)
5	−8.9	−10.0	Fe^{2+} (S_2)
6	−8.2	−4.8	$Fe^{2.5+}$ (S_1)
7	+6.9	+3.7	Fe^{2+} (S_1)
8	+7.7	+3.7	Fe^{2+} (S_1)

[a] This component has the value −8.1 MHz for Av. [b] Hyperfine coupling from ref 16 for which the sign as been changed.

7 and 8 with the ferrous pair of the $S_1 = {}^1/_2$ cubane, as shown on the final column of Tables 6 and 7.

From Tables 4 and 5, we see that the other iron expected to have a positive hyperfine parameter is the ferric ion of the $S_2 = {}^7/_2$ cubane and therefore the component (among components 3 to 6) for which we would like to propose a change of the sign of the hyperfine coupling for Cp should have a rather low isomer shift (and low ΔE_Q), compatible with a ferric character. Component 4 seems to be a good candidate, having an isomer shift of +0.25 well separated from all seven other components.

A reviewer has pointed out that this isomer shift is not well determined and could be as large as +0.41 mm/s as in the fit for the corresponding site from Av1 in the Zimmerman paper.[4] We note, however, that component 4 of both Cp1 and Av1 has a value of H_{int} that is considerably different from all other measured internal fields, as given in Table 3.[16] This site is clearly differentiated from other sites, and this, plus the low isomer shift and quadrupole splitting, is consistent with a trapped valence ferric site. (For example, the trapped ferric site within the $S = {}^7/_2$ cluster in $2[Fe_4Se_4]^+$ Cp ferredoxin[28] and has a measured isomer shift of 0.39 mm/s, within the 0.25−0.41 range.)

We can further extend the identification of the different components. Among components 3, 5 and 6 we expect one ferrous ion (the third of the $S_2 = {}^7/_2$ or ${}^5/_2$ cubane) and a mixed-valence pair. This ferrous ion seems most likely to be component 5 (relatively large isomer shift and quadrupole splitting), leaving components 3 and 6 as the mixed valence pair of the $S_1 = {}^1/_2$ cubane. The three ferrous ions of cubane 2 (components 1, 2, and 5) have, in our scheme, the three largest quadrupole splittings after components 7 and 8, assigned as ferrous sites of cubane 1. Their magnitudes range from +1.26 to +1.53 mm/s. It is interesting to note that, for the system $2[Fe_4Se_4]^+$ Cp Fd with spin ${}^7/_2$,[28] the three quadrupole splittings of the ferrous ions have been measured to be +1.67 mm/s, comparable to the values derived from our assignment for the ferrous ions in cubane 2. The complete result of our proposed assignment is presented in last column of either Tables 6 or 7.

To finish the discussion of the experimental data, let us consider the ZFS measurements obtained for P^{sOX} for Av.[24] This state P^{sOX} presents a spin ${}^7/_2$ signal[24] and yields a reasonable approximation for the value D_2 (ZFS parameter for cubane 2) in the state P^{OX}: $D_2 = -3.7 \pm 0.7$ cm^{-1}; for the sake of comparison, the value of D for the selenium-substituted cluster $[Fe_4Se_4]^+$ with spin ${}^7/_2$[27] is -2.1 ± 0.7 cm^{-1}. Finally, for P^{OX} itself, we have $D_t \approx -4$ cm^{-1} for the system *Xanthobacter autotrophicus*, Xal.[5] The ground doublet of this species has $g_{eff} = 15.6$, which is consistent with either an $S = 3$ or 4 spin multiplet. However, in the case of Av (also state P^{OX}), the EPR-active doublet is about 10−15 cm^{-1} above the ground-state,[5] and this gives a resonance transition with $g_{eff} = 11.9$. The species *Klebsiella pneumoniae*, Kp1, shows very similar resonance and temperature behavior to Av1. (In contrast, no EPR signal is observed for Cp1 at all, so it is difficult to draw any definite conclusions about the EPR of Cp1, except to rationalize this absence of a signal.) If we call $\mathbf{D}_1$ and $\mathbf{D}_2$ the ZFS tensors associated with cubanes 1 and 2 (with $\mathbf{D}_1 = 0$ when $S_1 = {}^1/_2$) in the state P^{OX}, and $\mathbf{D}_t$ the corresponding tensor for the

Table 8. a_{test} Values (MHz) for *C. pasteurianum* (Cp)

system	pattern	$S_t = 2$	$S_t = 3$	$S_t = 4$	$S_t = 5$
a_{test}[a]	6:2				
expt		−67.2	−44.8	−33.6	−26.9
a_{test}[b]	5:3				
expt		−46.3	−31.0	−23.2	−18.6
theory			−22.6[c]	−22.3[d]	
$\Sigma_{[-]}$, $\Sigma_{[+]}$[e]	5:3				
expt		−85.9, +39.6	−57.3, +26.3	−43.0, +19.8	−34.4, +15.8
theor			−44.3, +21.7[c]	−39.6, +17.3[d]	
$\Sigma_{[\text{cubane 1}]}$, $\Sigma_{[\text{cubane 2}]}$[f]	5:3				
expt		−3.9, −42.4	−2.7, −28.3	−2.0, −21.2	−1.6, −17.0
theory			−3.0, −19.6[c]	−2.6, −19.9[d]	

[a] Using the original experimental hyperfine parameters for Cp. For Av, we would have: −68.1, −45.5, −34.1, and −27.3 MHz, respectively. [b] Having changed the sign of the hyperfine parameter of component 4 (see text). For Av, we would have: −47.2, −31.7, −23.7, and −19.0 MHz, respectively. [c] For the state $|^1/_2, ^5/_2, 3\rangle$. [d] For the state $|^1/_2, ^7/_2, 4\rangle$. [e] Decomposition of the experimental a_{test} in negative ($\Sigma_{[-]}$) and positive ($\Sigma_{[+]}$) contributions. [f] Decomposition of the experimental a_{test} in cubanes 1 ($\Sigma_{[\text{cubane 1}]}$) and 2 ($\Sigma_{[\text{cubane 2}]}$) contributions.

whole P-cluster ($S_t = 3$ or 4), we can express $\mathbf{D}_t$ as a function of $\mathbf{D}_1$, $\mathbf{D}_2$, S_1, S_2, and S_t using the Wigner−Eckart theorem.[37] We find for the state $|^1/_2, ^7/_2, 3\rangle$ that $\mathbf{D}_t = +0.44\mathbf{D}_1 + 0.81\mathbf{D}_2$, for the state $|^1/_2, ^7/_2, 4\rangle$ that $\mathbf{D}_t = +0.29\mathbf{D}_1 + 0.46\mathbf{D}_2$, and for the state $|^1/_2, ^5/_2, 3\rangle$ that $\mathbf{D}_t = +0.24\mathbf{D}_1 + 0.43\mathbf{D}_2$. In every instance, since $\mathbf{D}_1 = 0$, the two tensors $\mathbf{D}_2$ and $\mathbf{D}_t$ are proportional. Using $\mathbf{D}_2 = -3.7 \pm 0.7$ cm^{-1}, we calculate for $\mathbf{D}_t$ respectively: -3.0 ± 0.6, -1.7 ± 0.3, and -1.6 ± 0.3 cm^{-1}. All three values are negative, in agreement with experiment, and the magnitude of D_t is almost twice as large for the state $|^1/_2, ^7/_2, 3\rangle$ (antiferromagnetic coupling between the halves) as for $|^1/_2, ^7/_2, 4\rangle$ and $|^1/_2, ^5/_2, 3\rangle$ (involving ferromagnetism). Now consider the possible state $|^1/_2, ^7/_2, 4\rangle$. An $S = 4$ ground state with $D < 0$ gives an $|M|_s = 4$ as the ground pseudodoublet and the $|M|_s = 3$ excited state at about $7|D|$ higher. The latter is expected to have a g_{eff} near 11.9, and with $D = -1.7$ cm^{-1}, this gives an excited doublet energy of about 12 cm^{-1}, which is in good agreement with the temperature dependence of the EPR from Av1 and Kp1. This analysis of the ZFS favors ferromagnetic coupling, which is the same conclusion we reached based on the signs of the hyperfine parameters of the ferrous ions. Also, an $S = 4$ spin multiplet is compatible with available EPR and Mössbauer data. Surerus et al. have shown[5] that the temperature dependent EPR spectra of Av1 and Kp1 are difficult to reconcile with Mössbauer spectroscopy when an $S = 3$ spin Hamiltonian is used. The problem is that when the ZFS parameter (E/D) is obtained which is consistent with the $g_{eff} = 11.9$ for an excited state pair, this (E/D) is much too large to be compatible with Mössbauer spectroscopy of the ground doublet. This is not a problem for an $S = 4$ multiplet, since (E/D) can be small for the $|M|_s = 3$ excited state resonance. Independent ways of testing the total spin and the spin coupling scheme are presented in the next section.

We cannot exclude the possibility of a quantum spin admixed ground state multiplet, so that the total spin S_t is not a good quantum number, but there is no strong evidence for this. The formalism for the connection between the measured internal magnetic fields and the hyperfine A values is the same, but S_t would represent the expectation value of the total spin, with a noninteger value between 3 and 4. We will explicitly consider only good spin quantum numbers for S_t, but the hyperfine analysis would not be greatly different for spin-admixed states. However, defining the character of a spin-admixed state based on Mössbauer and EPR spectroscopy in the P-clusters would be a formidable task.

(37) Scaringe, R. P.; Hodgson, D. J.; Hatfield, W. E. *Mol. Phys.* **1978**, *35*, 701−713.

V. Definition and Use of the Parameter a_{test}

Among the likely states for describing P^{ox}, those with antiferromagnetic coupling between the cubanes are inconsistent with the isomer shifts and corresponding signs of the hyperfine parameters. Can we go further and try to decide which of the two remaining candidate states—$|^1/_2, ^5/_2, 3\rangle$ and $|^1/_2, ^7/_2, 4\rangle$—is the most likely? In a recent analysis of hyperfine parameters in 1Fe, 2Fe, 3Fe, and 4Fe systems,[36] we defined a very simple and useful quantity called a_{test} as a function of the measured isotropic hyperfine coupling constants $A(\text{Fe}_i)$. We noticed that spin projection coefficients can be written as $K_i = [A(\text{Fe}_i)/a(\text{Fe}_i)]$. Since $\sum_i K_i = 1$, we defined the empirical quantity

$$a_{test} \equiv \sum_i A(\text{Fe}_i) \tag{7}$$

so that $\sum_i [A(\text{Fe}_i)/a_{test}] = 1$. As simple as this quantity may seem, it provides some useful insight into spin-coupling schemes for iron−sulfur clusters[36]. If a cluster is such that all the site values are expected to be the same (as in the cubane form of the $[Fe_3S_4]^+$ cluster[9,10] made formally of three ferric ions coupled to the total spin $^1/_2$), then a_{test} is the most useful estimate of the common site value, since it yields empirical spin projection coefficients summing up to 1 exactly.

When different site values are involved, a_{test} assumes a nontrivial variation through the alternation of positive and negative spin projection coefficients multiplied by site values of different magnitudes. This aspect of a_{test} is treated in more detail in ref 36. Here we estimate the value of a_{test} using the measured internal fields $H^i_{int} = +S_t A_{iz}/g_n\beta_n$. Since the magnitude of A_{iz} depends on S_t, so will a_{test}: $a_{test} = [g_n\beta_n/S_t]\sum_i H^i_{int}$. This is illustrated in the first line of Table 8 (case a) for the nitrogenase P-clusters of Av and Cp (within a 6:2 pattern), which gives a_{test} values for $S_t = 2$ to $S_t = 5$. The variation expected for such a quantity a_{test} is about 10%: this is typically what is observed for example for 4Fe ferredoxins (see Table 2) for which a_{test} varies around the mean value of −30.2 MHz by only ±10%. An alternative way to proceed is to follow the predictions of our theoretical analysis, that is a 5:3 pattern (Table 8, case b). In that case, one negative hyperfine constants would have been assigned with the wrong sign (we propose component 4). This change yields a_{test} values for which the appropriate changes of signs have been done, as reported in Tables 6 and 7. We now have $a_{test} \approx -31$ MHz for $S_t = 3$ and $a_{test} \approx -23$ MHz for $S_t = 4$.

We now estimate on theoretical grounds what values we expect for a_{test}. It is clear, of course, that the 5:3 and 6:2 patterns will not have a priori the same value of a_{test}: the value we would get for the 6:2 pattern directly from the experimental data is

necessarily more negative than the one derived for the 5:3 pattern, obtained by changing one negative sign, as is obvious from the definition of the quantity a_{test}. Therefore, within the working hypothesis of a 5:3 pattern, we would like to know which of the two states $|^1/_2, {}^5/_2, 3\rangle$ or $|^1/_2, {}^7/_2, 4\rangle$ is the more likely, based on the dependence of a_{test} on S_t. There are two ways to proceed, in exact analogy with our estimates of the hyperfine parameters. Using the data in Table 2, we can compute a_{test} for a "classic" reduced 4Fe ferredoxin of spin $^1/_2$ and $^7/_2$:

$$\begin{cases} a_{test}(S_1 = {}^1/_2) \approx -30 \text{ MHz} \\ a_{test}(S_2 = {}^7/_2) \approx -23 \text{MHz} \end{cases} \tag{8}$$

We can then estimate what value of a_{test} to expect for the whole cluster in the same way as we estimated hyperfine parameters for P^{OX} from the knowledge of the corresponding couplings for "isolated" 4Fe reduced ferredoxins. We consequently couple $^1/_2$ and $^7/_2$ to $S_t = 3$ or $S_t = 4$, and we obtain $a_{test}(|^1/_2, {}^7/_2, 3\rangle)$ and $a_{test}(|^1/_2, {}^7/_2, 4\rangle)$ in the following manner:

$$\begin{cases} a_{test}(|^1/_2, {}^7/_2, 3\rangle) = (-{}^1/_8)a_{test}(S_1 = {}^1/_2) + \\ \qquad\qquad ({}^9/_8)a_{test}(S_2 = {}^7/_2) \approx -22 \text{ MHz} \\ a_{test}(|^1/_2, {}^7/_2, 4\rangle) = (+{}^1/_8)a_{test}(S_1 = {}^1/_2) + \\ \qquad\qquad ({}^7/_8)a_{test}(S_2 = {}^7/_2) \approx -24 \text{ MHz} \end{cases} \tag{9}$$

Since the spin coupling coefficients associated with the cubane of spin $S_1 = {}^1/_2$ are small ($\pm{}^1/_8$), the value of a_{test} for the whole P-cluster is essentially determined by that of the cubane with larger spin (here $S_2 = {}^7/_2$). Moreover, these calculated a_{test} values do not show a marked variation on S_t. Our predicted value is hence around -23 MHz. For this estimate, it will be noticed that we have not assumed anything about the magnitudes of the site values $a(Fe_i)$ for the two cubanes.

As a test of the robustness of the definition of the quantity a_{test}, we can also estimate its value from the calculated hyperfine parameters of Table 5, which are based on assumed site values $a(Fe_i)$. From $a_{test} = \sum_i K_i a(Fe_i)$, we obtain

$$\begin{cases} a_{test}(|^1/_2, {}^7/_2, 3\rangle) \approx -24 \text{ MHz} \\ a_{test}(|^1/_2, {}^7/_2, 4\rangle) \approx -22 \text{ MHz} \\ a_{test}(|^1/_2, {}^5/_2, 3\rangle) \approx -23 \text{ MHz} \end{cases} \tag{10}$$

The conclusion is the same as above, regarding the magnitude of a_{test}: whatever the state we consider, the value of a_{test} is confined within the range -22 to -24 MHz. This suggests that we should expect a_{test}, calculated from the experimental internal field (H_{int}) data, to fall close to -23 MHz. The empirical values of a_{test} reported in Table 8 indicate that the case for which $S_t = 4$ (associated with a 5:3 pattern) is the most probable. In Table 8, we decompose a_{test} in two ways, first considering the sum of the positive and negative contributions and then considering the partial sums over the two cubanes. In every instance, a value of 4 for S_t appears by far the most likely case, in agreement with a parallel spin orientation of the two clusters.

These remarks lead us to the conclusion that the correct spin state describing the spin coupling in a P-cluster in the oxidation state P^{OX} is most likely $|^1/_2, {}^7/_2, 4\rangle$. We present in the Appendix an analysis of the consequences we can derive from a 6:2 pattern for the signs and magnitudes of the hyperfine parameters (as originally proposed[4,16]). We find that a 6:2 pattern represents a poorer fit between experimental data and theoretical models than 5:3, and therefore 6:2 is improbable.

The coupling between neighboring iron ions in iron–sulfur systems is usually antiferromagnetic (rationalized by invoking dominant superexchange[38] pathways via the bridging sulfur ligands[39]). We show in Figure 1 that such a constraint can be respected while having the spins S_1 and S_2 associated with the halves of the P^{OX}-cluster coupled ferromagnetically. We identify the iron nearest to the serine residue as the trapped ferric ion. This determines that the cubane to which that ferric ion belongs has a subspin S_2 of $^7/_2$. The two irons facing the other cubane are therefore ferrous in character and define, with the third ferrous ion, the direction of S_2. In our scheme, cubane 1 of spin $S_1 = {}^1/_2$ is made of a ferrous pair and a delocalized mixed-valence pair. The spin S_1 is aligned with that of the mixed-valence pair and therefore with S_2. To optimize the number of antiferromagnetic interactions between pairs of ions, we would place the ferrous pair of cubane 1 close to those of cubane 2, as depicted in Figure 1.

This model for the redox state P^{OX} also allows us to gain some insight into the state P^N. It has been shown that the total absorption of the signals 7 and 8 (in the state P^{OX}) and signal "Fe^{2+}" (in the state P^N) is constant during a thionine oxidation titration of the Av MoFe protein,[4] starting from P^N. Furthermore, the sum of the absorption of both components 7 and 8 ($13 \pm 0.6\%$) matches exactly that of component "Fe^{2+}" (found to be 13%),[4] which is what would be expected if the signal "Fe^{2+}" transforms into signals 7 and 8 upon oxidation from P^N to P^{OX} (the absorption is taken as a percentage of the total iron content, thus including both P and M clusters). In the state P^N, in addition to the signals called D, a component called S ($\Delta E_Q = 1.4$ mm/s and $\delta = 0.6$ mm/s) was also detected for Av.[3,40] It was then shown, by highly resolved Mössbauer studies of the MoFe protein of *K. pneumoniae*, that component S belongs to the P-cluster.[33] The Fe^{2+}:D:S ratio is 2:5:1 at 4.2 K, so expressed so as to sum to eight irons. Within the working hypothesis that the (4Fe) P-clusters appeared in two inequivalent pairs, it was then proposed that one cluster would be of the type [D_3, Fe^{2+}] and the other of the type [D_2, S, Fe^{2+}]. Knowing now that a P-cluster contains 8Fe, our analysis presented above of the hyperfine parameters for the state P^{OX} would lead us to another distribution of the components "Fe^{2+}", D, and S in the state P^N. Components 7 and 8 in P^{OX} are located in cubane 1, facing the interior of the P-cluster, and therefore the two components "Fe^{2+}" most probably occupy the same location in P^N. Among the six remaining iron sites, five are tetracoordinated to sulfurs, among which we would expect a priori a 2:2:1 pattern (2D:2D′:D″), that is 2[exterior ions of cubane 1]:2[interior ions of cubane 2]:1[ion coordinated to $cys^{\beta 70}$]. The sixth site, component S (previously the ferric ion in the state P^{OX}), has an extra coordination with the serine. The whole could be simplified into a 5:1 pattern for the six remaining ferrous components of the state P^N, that is five D and one S, if we identify component S with the pentacoordinated iron. This results in one cluster of the type [D_2, Fe_2^{2+}] (for cubane 1) and the other of the type [D_3, S] (for cubane 2).

VI. Conclusions

Our goal in this study was to obtain some insight into the spin coupling scheme adopted by a P-cluster (in Cp and Av) in

(38) (a) Anderson, P. W. *Phys. Rev.* **1959**, *115*, 2. (b) Anderson, P. W. In *Solid States Physics*; Seitz, F., Turnbull, D., Eds.; Academic: New York, 1963; Vol. 14, pp 99–214. (c) Hay, P. J.; Thibeault, J. C., Hoffmann, R. *J. Am. Chem. Soc.* **1975**, *97*, 4884–4899.

(39) (a) Noodleman, L. *J. Chem. Phys.* **1981**, *74*, 5737–5743. (b) Noodleman, L.; Baerends, E. J. *J. Am. Chem. Soc.* **1984**, *106*, 2316–2327.

(40) Huynh, B. H.; Münck, E.; Orme-Johnson, W. H. *Biochim. Biophys. Acta* **1979**, *527*, 192–203.

Table 9. Summary of Our Analysis

state	criterion: ferro.	criterion: a_{test}	criterion: pattern[a]
$\|1/2, 7/2, 3\rangle$	no	no	5:3
$\|1/2, 7/2, 4\rangle$	yes	yes	5:3
$\|1/2, 5/2, 3\rangle$	yes	no	5:3
$\|3/2, 7/2, 3\rangle$	no	no	3:1[b]
$\|3/2, 7/2, 4\rangle$	yes	yes	7:1
$\|3/2, 5/2, 4\rangle$	yes	yes	7:1

[a] In the order negative:positive hyperfine parameters. [b] The four predicted hyperfine parameters of cubane 1 are zero.

its P^{OX} oxidation state. For that we first worked out, based on Mössbauer data and EPR studies, what we should expect for the formal composition of the two "cubanes" composing a P-cluster. We started with the remark that the state P^N appears to be "all ferrous" (and EPR silent) and ended with the following points.

(a) P^{OX}, obtained from P^N by a two-electron oxidation, is made of two pseudocubanes, each formally analogous to a $[Fe_4S_4]^+$ cluster (charge counted as if this 4Fe cluster were isolated as in "classic" ferredoxins).

(b) One half of the P^{OX}-cluster has a spin $1/2$ whereas the other has a spin $7/2$. This differentiation between the halves may be related to the presence of a serine residue coordinated to the ferric site of the $7/2$.

(c) The hyperfine coupling constants appear in a 5:3 pattern (five negative and three positive values) as a consequence of coupling either ferromagnetically or antiferromagnetically the spin $1/2$ and spin $7/2$ of the halves of a P-cluster. An analysis of the magnitude of the quantity a_{test} for the two patterns 6:2 and 5:3 strongly favors the latter.

(d) The total spin S_t of the P^{OX}-cluster is 4 (rather than 3). This identification was reached in two independent ways. We started with the six possible spin states shown in Table 9. First, the last three states were discarded because they present only one positive hyperfine coupling constant (at least two were measured experimentally for Av and Cp). Then we considered components 1, 2, 7, and 8 for both Av and Cp (all ferrous ions according to their isomer shift measurements) for which the observed two positive and two negative hyperfine parameters are compatible only with ferromagnetism; this eliminates the state $|1/2, 7/2, 3\rangle$. Finally we defined the quantity a_{test} and compared it with predicted values derived from the spin projection coefficients associated with the states listed above. This supported our suggested assignment of $|1/2, 7/2, 4\rangle$ over other possible coupling schemes. The predicted $A(Fe_i)$ values from our spin coupling model are in good agreement with observed values provided one hyperfine sign is changed. Further, such changes make the hyperfine patterns similar to that expected for the state with $S_t = 4$. We propose that the fitting procedure applied to Av and Cp be reinvestigated to see if a 5:3 pattern would not be as good or better than the 6:2 pattern.

(e) Our analysis and results for the redox state P^{OX} allowed us to make some suggestions regarding the assignments of the components "Fe^{2+}", D, and S in the state P^N and to rationalize observed features of the P^{pOX} and P^{sOX} states.

These assignments for the total cluster spin ($S_t = 4$), the pattern of hyperfine parameters (equivalently the spin vector alignment), and the locations of the ferrous, mixed-valence, and ferric sites are testable by various methods: (1) more detailed EPR at various frequencies to determine the g_{eff} for different pseudodoublets and finally S_t; (2) further measurements and analysis of fits to Mössbauer hyperfine data along with quadrupole splitting and isomer shift information; (3) site directed mutagenesis at the serine to see if this can disrupt the stability of the $S_2 = 7/2$ cubane and the ferric character of the coordinated iron site; (4) mutagenesis of the bridging cysteines to see the effects on the individual cubanes and their subsequent spin coupling.

Table 10. Spin States of 4Fe Reduced Ferredoxins

tot. spin	state	pattern	$K(Fe^{2+})$	$K(Fe^{2+})$	$K(Fe^{2+})$	$K(Fe^{3+})$
$S = 1/2$	$\|9/2, 4, 1/2\rangle^a$	2:2	−1.333	−1.333	+1.833	+1.833
	$\|7/2, 3, 1/2\rangle^a$	2:2	−1.000	−1.000	+1.500	+1.500
$S = 3/2$	$\|4, 2, 3/2\rangle^b$	4:0	+0.111	+0.111	+0.389	+0.389
$S = 5/2$	$\|4, 5, 5/2\rangle^b$	3:1	+0.629	+0.629	+0.457	−0.714
	$\|4, 2, 5/2\rangle^b$	3:1	+0.286	+0.286	−0.229	+0.657
$S = 7/2$	$\|4, 6, 7/2\rangle^b$	3:1	+0.519	+0.519	+0.519	−0.556
$S = 9/2$	$\|1/2, 4, 9/2\rangle^c$	3:1	+0.444	+0.444	−0.148	+0.259

[a] State $|S(2Fe^{2.5+}), S(2Fe^{2+}), S\rangle$. [b] State $|S(2Fe^{2+}), S^*, S\rangle$. [c] State $|S(Fe^{2+}-Fe^{3+}), S(2Fe^{2+}), S\rangle$.

From the viewpoint of biological activity, the presence of the serine and the trapping of Fe^{3+} in P^{OX} is fascinating. Is the serine always coordinated to the cluster, or does coordination occur on $P^N \rightarrow P^{OX}$ oxidation? Is the serine deprotonated throughout, or does deprotonation accompany oxidation? Further, we note that our proposed model has the Fe^{3+} and the mixed-valence $Fe^{2.5+}-Fe^{2.5+}$ pair in P^{OX} facing the outside of the 8Fe structure while four of the five Fe^{2+} sites face the interior (bridging cysteines and the disulfide bond). This suggests that oxidation of the 8Fe occurs preferentially at the outer sites, although considerable delocalization of charge throughout the structure is expected as found in cubane systems.[41]

Acknowledgment. We thank B. Lamotte for helpful discussions and Doug Rees for providing coordinates from the X-ray model for the P-cluster. This work was supported by NIH Grant GM39914 and by a NATO travel grant to D.A.C., L.N., and B. Lamotte. J.M.M. gratefully acknowledges additional financial support from the French Ministry of Foreign Affairs through the Lavoisier Grant (for the period December 1, 1991, through December 1, 1992).

Appendix: Implications of a 6:2 Pattern (Signs of the Hyperfine Parameters) for the Ground State of P^{OX}

In this appendix, we want to show why a 5:3 pattern for the signs of the hyperfine parameters is more likely to occur than a 6:2 pattern. We assume here this 6:2 pattern and try to deduce what spin states are compatible with that hypothesis. Let us note at first that the two positive components observed for the state P^{OX} are 7 and 8 (see Table 3). The corresponding isomer shifts are visibly ferrous in character. The six remaining (and negative) components correspond therefore to four ferrous and two ferric ions: we assumed that, in the redox state P^N, all the ions are ferrous and, therefore, the state P^{OX} consists of two formal $[Fe_4S_4]^+$ clusters, each containing three ferrous ions and one ferric ion. To allocate one ferric ion to each of the two cubanes is the only way to have half-integer spins S_1 and S_2 for each of them. According to Table 2 (and also the theoretical work done for 4Fe reduced ferredoxins[15]), we know what are the patterns and states to expect for each cubane. These are listed in Table 10 (since the site values are negative, the signs of the spin projection coefficients are opposite to those of the hyperfine parameters).

We have only two possibilities: the two components 7 and 8 (ferrous ions) are located on the same cubane (either cubane 1 or cubane 2), or each of the two cubanes contains one of them. In the first case, the only possible pattern (within the

(41) Noodleman, L.; Norman, J. G. Jr.; Osborne, J. H.; Aizman, A.; Case, D. A. *J. Am. Chem. Soc.* **1985**, *107*, 3418−3426.

constraint that their hyperfine parameters are positive, or that the corresponding spin projection coefficients are negative) is (2:2) for cubane 1 and (4:0) for cubane 2, according to Table 10. This means that we can only couple a spin $^1/_2$ with a spin $^3/_2$, resulting in a value of S_t of 1 or 2, which is excluded ($S_t \geq 3$). Consequently, the two positive components 7 and 8, within a (6:2) pattern for the whole cluster, have to belong each to one cubane (in contrast to the case of a 5:3 pattern, which led us to locate these two ferrous ions in cubane 1). Within this hypothesis, the 6:2 pattern for the P-cluster (where the two positive hyperfine values, or equivalently the two negative spin projection coefficients, are on ferrous sites) has to be decomposed into (3:1)(3:1), that is only the states (for a cubane) $|4, 2, {}^5/_2\rangle$ and $|{}^1/_2, 4, {}^9/_2\rangle$ have to be considered, according to Table 10. Note also that only positive values of K^q, $q = 1, 2$, are allowed given the 6:2 pattern.

Some important features of a_{test} aid the selection process. We have seen, from Table 2, that a_{test} is limited to the range -15 to -36 MHz (or -23 to -34 MHz if we discard the measurements done for the $S = {}^3/_2$ systems due to possible large uncertainties). If one thinks of a_{test} as $\sum_i K_i a(\mathrm{Fe}_i)$, it is possible to relate the difference between the average value of a_{test} for $S = {}^1/_2$ systems (≈ -30 MHz) and the same quantity for $S = {}^7/_2$ systems (≈ -23 MHz) to a smaller value of $a(\mathrm{Fe}^{2+})$ for the former (we found, in ref 36, that $a(\mathrm{Fe}^{2+}) \approx -18$ MHz for $[\mathrm{Fe_4S_4}]^+$ systems, rather than -22 MHz in the case of reduced rubredoxins). There are then some variations among the site values. It is clear however from the very definition of $a_{test} = [\sum_i K_i a(\mathrm{Fe}_i)]/[\sum_i K_i]$ that a_{test} is a weighted average of the site values $\{a(\mathrm{Fe}_i)\}$, and consequently its range is intrinsically limited. This is illustrated in Table 2 for example, where different systems present comparable a_{test} values, or in Tables 5 and 11 in which a common set of $\{a(\mathrm{Fe}_i)\}$ used in conjunction with different spin projection coefficients yields very similar a_{test} values (ranging from -20 to -24 MHz). We conclude therefore that a_{test} for P^{ox} should be expected to be limited within a certain range (typically $|a_{test}| < 40$ MHz, which is conservative). Table 8 gives the values of a_{test}, for a 6:2 pattern, in the cases $S_t = 2-5$. Only $S_t = 4$ or 5 seem reasonable ($a_{test} \approx -45$ for $S_t = 3$). Therefore, when we consider different coupling schemes for the P-cluster involving, for the individual cubanes, the states $|4, 2, {}^5/_2\rangle$ and $|{}^1/_2, 4, {}^9/_2\rangle$, we propose to construct the six states ($|S_1, S_2, S_t\rangle$), listed in Table 11.

Table 11. Predicted Hyperfine Parameters for a 6:2 Pattern[a]

	cubane 1		cubane 2		
$\|S_1, S_2, S_t\rangle$	K^1	$(3Fe^{2+},Fe^{3+})$	K^2	$(3Fe^{2+},Fe^{3+})$	a_{test}
$\|{}^5/_2, {}^5/_2, 4\rangle$	$^1/_2$	(−3.1, −3.1, +2.5, −6.5)	$^1/_2$	(−3.1, −3.1, +2.5, −6.5)	−20.4
$\|{}^5/_2, {}^9/_2, 4\rangle$	$^1/_{10}$	(−0.6, −0.6, +0.5, −1.3)	$^9/_{10}$	(−8.8, −8.8, +3.0, −4.7)	−21.3
$\|{}^9/_2, {}^9/_2, 4\rangle$	$^1/_2$	(−4.9, −4.9, +1.6, −2.6)	$^1/_2$	(−4.9, −4.9, +1.6, −2.6)	−21.6
$\|{}^5/_2, {}^5/_2, 5\rangle$	$^1/_2$	(−3.1, −3.1, +2.5, −6.5)	$^1/_2$	(−3.1, −3.1, +2.5, −6.5)	−20.4
$\|{}^5/_2, {}^9/_2, 5\rangle$	$^7/_{30}$	(−.1.5, −1.5, +1.2, −3.1)	$^{23}/_{30}$	(−7.5, −7.5, +2.5, −4.0)	−21.4
$\|{}^9/_2, {}^9/_2, 5\rangle$	$^1/_2$	(−4.9, −4.9, +1.6, −2.6)	$^1/_2$	(−4.9, −4.9, +1.6, −2.6)	−21.6

[a] The experimental values (listed from components 1 to 8) in the case $S_t = 4$ (from Table 7) and $S_t = 5$ are, respectively, as follows: (−9.9, −7.6, −8.4, −5.2, −8.9, −8.2, +6.9, +7.7) and (−7.9, −6.1, −6.7, −4.1, −7.1, −6.5, +5.5, +6.1).

Most of these states are "canted" spin states (especially when $|{}^1/_2, 4, {}^9/_2\rangle$ is involved). We then calculated, for each of these states, the corresponding spin projection coefficients and predicted hyperfine parameters, using eq 5 and the same set of site values as in the main text. The coefficients $\{K^q\}$ (from the projection of the cubane spin S_q onto the total spin S_t) and the hyperfine couplings are listed in Table 11. We notice at first that the predicted values of a_{test} are all between -20 and -22 MHz, reenforcing our previous analysis regarding the selection of possible S_t values on the basis of calculated a_{test} values as presented in Table 8. Notice that the experimental a_{test} amounts to -33.6 MHz ($S_t = 4$) for a 6:2 pattern, which is much higher than the theoretical a_{test}. Second, most of the calculated hyperfine parameters are too small to compare well with the experimental data (see Table 7 for the case $S_t = 4$). With $S_t = 5$, we would have from the experimental data (for component 1 to 8 for Cp): -7.9, -6.1, -6.7, -4.1, -7.1, -6.5, $+5.5$, and $+6.1$. We obtained a much better agreement when we considered a 5:3 pattern for the signs of the hyperfine parameters. A 5:3 pattern then appears more likely than a 6:2 pattern.[16]